The Holocene 16,4 (2006) pp. 467–477

Modelling river discharge and precipitation from estuarine salinity in the northern Chesapeake Bay: application to Holocene palaeoclimate

Casey Saenger,[1]* Thomas Cronin,[2] Robert Thunell[3] and Cheryl Vann[2]

([1]Massachusetts Institute of Technology, E34-205, Cambridge MA 02139, USA; [2]M.S. 926a U.S. Geological Survey National Center, Reston VA 20192, USA; [3]Department of Geoscience, University of South Carolina, Columbia SC 29208, USA)

Received 21 December 2004; revised manuscript accepted 24 November 2005

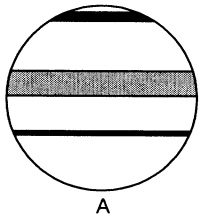

Abstract: Long-term chronologies of precipitation can provide a baseline against which twentieth-century trends in rainfall can be evaluated in terms of natural variability and anthropogenic influence. However, there are relatively few methods to quantitatively reconstruct palaeoprecipitation and river discharge compared with proxies of other climatic factors, such as temperature. We developed autoregressive and least squares statistical models relating Chesapeake Bay salinity to river discharge and regional precipitation records. Salinity in northern and central parts of the modern Chesapeake Bay is influenced largely by seasonal, interannual and decadal variations in Susquehanna River discharge, which in turn are controlled by regional precipitation patterns. A power regressive discharge model and linear precipitation model exhibit well-defined decadal variations in peak discharge and precipitation. The utility of the models was tested by estimating Holocene palaeoprecipitation and Susquehanna River palaeodischarge, as indicated by isotopically derived palaeosalinity reconstructions from Chesapeake Bay sediment cores. Model results indicate that the early–mid Holocene (7055–5900 yr BP) was drier than the late Holocene (1500 yr BP – present), the 'Mediaeval Warm Period' (MWP) (1200–600 yr BP) was drier than the 'Little Ice Age' (LIA) (500–100 yr BP), and the twentieth century experienced extremes in precipitation possibly associated with changes in ocean–atmosphere teleconnections.

Key words: Chesapeake Bay, palaeoclimate, palaeoprecipitation, palaeohydrology, salinity, Susquehanna River, teleconnections, Holocene.

Introduction

Historical patterns of precipitation (Karl *et al.*, 1995) and climate model simulations (Cohen and Miller, 2001) suggest that twentieth century rainfall in North America has experienced anomalous, generally increasing, behaviour that has been partly attributed to the influence of anthropogenic trace gases on atmospheric circulation. However, because of the relatively short period of instrumental records (~ 100 years), it is not clear how much of this variability is part of natural decadal and centennial climate variability and how much is human-induced. Palaeoclimate records can provide quantitative data on long-term precipitation variability that serves as a baseline against which twentieth century trends can be compared, but quantitative methods to estimate past rainfall over millennial timescales are relatively few.

In addition to sedimentary records from lakes, which record rainfall-driven changes in lake levels and chemistry (Laird *et al.*, 1996), estuaries also offer a potentially untapped source of palaeoprecipitation records. Rainfall and freshwater discharge are often the predominant factors influencing estuarine salinity, especially where there is little evaporation. Moreover, historical records of the past 60 years show that relatively small interannual changes in precipitation (~ 10%) can be amplified by a factor of two in terms of their impact on streamflow (Karl and Riebsame, 1989; Najjar, 1999). Perhaps more importantly,

*Author for correspondence (e-mail: csaenger@mit.edu)

10.1191/0959683606hl944rp

palaeoenvironmental studies of San Francisco Bay (Cayan and Peterson, 1993; Peterson *et al.*, 1995; Ingram *et al.*, 1996), Chesapeake Bay (Cronin *et al.*, 2000) and Florida Bay (Swart *et al.*, 1996; Dwyer and Cronin, 2001) have shown that large-scale, climate-driven fluctuations in salinity exist over the past millennium and that some salinity extremes have exceeded those seen in historical instrumental records. Furthermore, changes in Chesapeake Bay temperature have been attributed to the influence of atmosphere–ocean coupling on surface temperatures and thermohaline circulation in the North Atlantic Ocean (Cronin *et al.*, 2003), suggesting salinity, discharge and precipitation may also be influenced by large-scale atmospheric and oceanic teleconnections. Developing quantitative long-term palaeoprecipitation records is particularly important for the eastern USA because tree-ring (Cook and Jacoby, 1983; Stahle *et al.*, 1998; Druckenbrod et al., 2003) and sediment core records (Cronin *et al.*, 2000) indicate that periods of extreme drought and wet climate have punctuated the last few centuries.

Chesapeake Bay, the largest estuary in the USA (Figure 1), is especially suitable for investigations of long-term, eastern US precipitation trends because of the relationship between Susquehanna River freshwater discharge and bay salinity (Figure 2). This relationship is strongest in the upper bay, defined here as the portion of the bay north of the Potomac River estuary. In this region, Susquehanna River freshwater inflow and the effects of tides primarily control salinity, and inflow from smaller tributaries is minimal (Schubel and Pritchard, 1986). Freshwater inflow from the Susquehanna River, the largest river discharging into the bay, is in turn highly correlated ($r^2 = 0.90$) with regional precipitation on the annual timescale (Najjar, 1999). This paper complements previous regional models[1] by presenting quantitative models relating instrumental measurements of Chesapeake Bay salinity, Susquehanna River discharge and regional precipitation. Models presented here are designed to infer quantitative reconstructions of long-term freshwater inflow and regional precipitation from proxy records of Holocene salinity changes obtained from oxygen isotope analyses ($\delta^{18}O$) of calcareous ($CaCO_3$) fossil foraminifera shells described in Cronin *et al.*, (2005). Although the models described below are applicable to the mid-Atlantic region of eastern North America, we believe the methodology can be extended to most estuaries and coastal systems characterized by salinity variability and Holocene sediment accumulation.

Regional setting

The Chesapeake Bay trends ~300 km north–south with a surface area of 6500 km^2 and a watershed of 166000 km^2 (Schubel and Pritchard, 1986) (Figure 1). The Susquehanna River is a major tributary of the bay, and drains a watershed of 71 250 km^2 in Maryland, Pennsylvania and New York with an average monthly discharge of ~1100 m^3 (Schubel and Pritchard, 1986). The bay is a partially mixed, stratified estuary with two-way circulation that creates a strong, seaward-increasing, salinity gradient in both surface and bottom waters

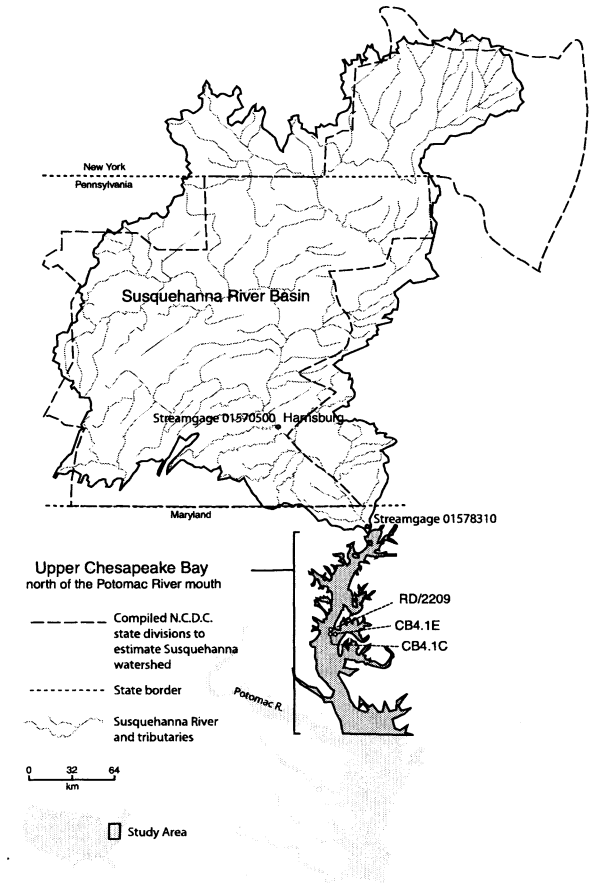

Figure 1 Susquehanna River drainage basin (bold line) and the Chesapeake Bay with the northern portion considered in this study marked in bold. CB4.1C and CB4.1E mark instrumental salinity sites, and RD/2209 is a foraminiferal $\delta^{18}O$-derived palaeosalinity record (Cronin *et al.*, 2005). Modelled discharge was compared with instrumental data from USGS streamguages 01570500 (Harrisburg) and 01578310 (Conowingo). Modelled precipitation was compared with watershed precipitation records estimated from six NCDC state divisions (long dashed line)

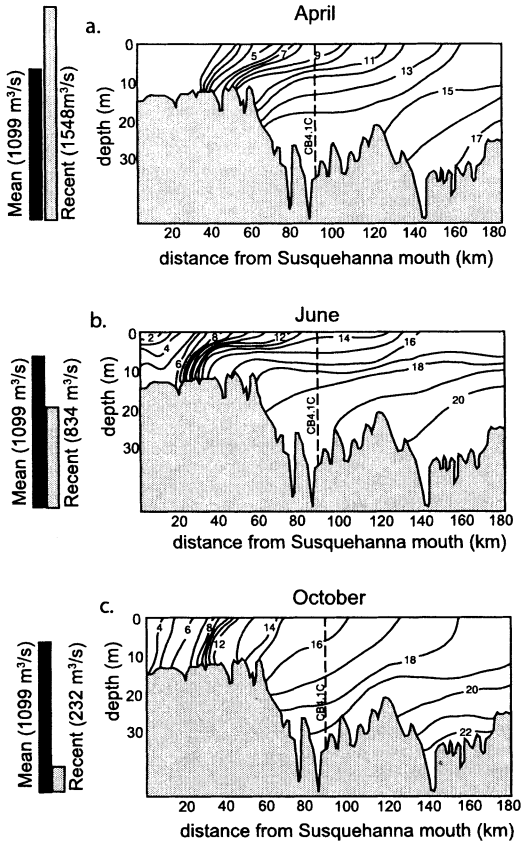

Figure 2 Variability of salinity with discharge in the upper 180 km of the Chesapeake Bay. Salinity at station CB4.1C shows a strong response to seasonal variation with Susquehanna discharge. Long-term mean Susquehanna discharge (dashed column) is compared with the recent discharge (solid column) averaged over the ten days preceding the salinity shown in the accompanying diagram. (a) Above average April discharge pushes isohalines south toward the bay mouth, (b) lower discharge summer months exhibit stronger vertical stratification; (c) below average autumn discharge causes a northward retreat of isohalines toward the Susquehanna River mouth. Adapted from Schubel and Pritchard (1986). Reproduced with the permission of the Estuarine Research Federation

(Schubel and Pritchard, 1986) (Figure 2). Salinity shows a strong response to Susquehanna River discharge, which supplies 87% of the freshwater to the upper bay, north of the Potomac River mouth (Schubel and Pritchard, 1986). Higher Susquehanna discharge results in strengthened vertical stratification and a southward shift of isohalines toward the bay mouth. Seasonal salinity extremes in the upper bay range from 0 to > 22 ppt, and are related to seasonal variability in Susquehanna River discharge. Discharge reaches a maximum in early spring associated with snow melt and spring rains, and generally exhibits low to moderate flow through the remainder of the year (Schubel and Pritchard, 1986). Similarly, discharge is primarily controlled by Susquehanna watershed precipitation, which ranges from 80 to 130 cm/yr and exhibits a weak annual cycle with greatest values in early summer and lower winter values (Najjar, 1999). Annual decoupling between discharge and precipitation, not apparent over interannual timescales, is attributed to seasonal variations in evapotranspiration, and to the effects of storage associated with snow accumulation (Najjar, 1999).

Precipitation in the middle-Atlantic USA is strongly influenced by the shape of troposhperic circulation and the position of the circumpolar jet stream (Vega *et al.*, 1998, 1999). Circulation varies from zonal flow, with a flattened circumpolar jet, to meridional flow, which is marked by an enhanced ridge and trough structure. During periods of meridional circulation, the precise position of the jet stream trough determines precipitation receipt (Yarnal and Leathers, 1988), and a westward displaced trough is associated with a storm track that parallels the Atlantic coast of the USA, while a more easterly trough exhibits a storm track that follows the Gulf Stream offshore (Resio and Hayden, 1975; Bradbury *et al.*, 2002). The North Atlantic Oscillation (NAO), defined as the sea level pressure (SLP) gradient between Iceland and the Azores, is a major source of changes in atmospheric circulation over multiannual timescales (Hurrell, 1995), and potentially alters precipitation within the Susquehanna River watershed. In the Pacific Ocean, the Pacific North American (PNA) teleconnections pattern is marked by variations in geopotential height anomalies between Hawaii and Alberta, and the Aleutian Low and Florida (Wallace and Gutzler, 1981), while the North Pacific Mode (NPM) is characterized by strong sea-surface temperature (SST) anomalies within the Aleutian low (Barlow *et al.*, 2001). Decadal variability in these patterns also potentially influences precipitation over the Susquehanna River watershed by modulating the degree of zonal versus meridional atmospheric circulation (Vega *et al.*, 1999; Sheridan, 2003). The sensitivity of precipitation in the northern Chesapeake Bay to changes within coupled ocean–atmosphere circulation make it a uniquely valuable site in which to develop reconstructions of palaeoprecipitation.

Materials and methods

In order to develop a method of quantifying past regional precipitation trends, we first compiled and analysed relationships between instrumental Chesapeake Bay salinity and Susquehanna discharge data. We then evaluated the quantitative relationships between instrumental records of freshwater discharge and regional precipitation. These relationships were verified and evaluated using independent instrumental data, and the most appropriate salinity–discharge and discharge–precipitation models were selected based on the verification results.

A salinity–discharge model was then applied to a reconstruction of Holocene salinity developed from benthic foraminiferal oxygen isotopic records in Chesapeake Bay sediment cores discussed in depth in a parallel study (Cronin *et al.*, 2005). The computation of palaeosalinity relies on the fact that the oxygen isotope composition of Chesapeake Bay water is positively correlated with salinity, and represents a mixing of isotopically depleted and enriched, fresh and marine, end members. Foraminifera secrete a calcareous ($CaCO_3$) shell in which the oxygen isotopic ratio is influenced by salinity and water temperature (Epstein *et al.*, 1953; Broecker, 1989). By factoring out the influence of water temperature using independent palaeotemperature estimates based on ostracode magnesium/calcium ratios, a record of palaeosalinity can be recovered (Cronin *et al.*, 2005). Applying this approach to a sediment core record located in the upper bay (RD/2209, Figure 1), which contains an excellent isotopic record for the middle to late Holocene, we computed palaeodischarge from the salinity–discharge model and then input palaeodischarge into the discharge–precipitation model to estimate Holocene trends in rainfall.

The salinity input for the salinity–discharge model was obtained from the 17-yr (1985–2001) salinity record from

Chesapeake Bay Program (CBP) monitoring station CB4.1C, located adjacent to RD/2209 (Figure 1).[1] This station captures seasonal and interannual salinity variability at a monthly (submonthly for spring–autum months) resolution, as well as salinity changes in the water column. We chose to construct salinity–discharge models from two water depths – below 20 m and below 30 m – because the foraminifera *Elphidium* used for isotopic palaeosalinity computations are bottom-dwelling in habitat, and RD/2209 was recovered from a water depth of 20–25 m.

Monthly salinity means were calculated for each month at the two depth zones from January to December (annual), and during the spring season, with separate spring monthly mean values evaluated for March–June (MAMJ), May–June (MJ), May and June. All values indicate a monthly value, for example, MAMJ averages the four individual March, April, May and June mean monthly values for a given year. We focused on the spring season because this is generally the time of peak discharge and precipitation, and is also likely the time when most benthic foraminifera secrete their shells. The water year has been shown to have a weaker correlation with river discharge (Najjar, 1999), and was not considered here.

An independent instrumental salinity record, dating from 1950 to 1979, was obtained from the Chesapeake Bay Institute (CBI) data bank[1] and was used to verify the salinity–discharge relationship. Salinity data for this period were averaged from nine mid-bay monitoring sites located within 30 km of the sediment core RD/2209. The pooled salinity from these sites generally captures salinity fluctuations occurring on monthly scales. We then separated the salinity record into annual, MAMJ, MJ, May and June temporal divisions, and into spatial divisions below 20 m and below 30 m water depth to correspond with the CB4.1C record.

US Geological Survey (USGS) streamguage records of Susquehanna discharge from Conowingo, Maryland (station 01578310) and Harrisburg, Pennsylvania (station 01570500)[1] were analysed. These data account for small discharge variations associated with flood control and hydroelectric reservoirs by minimal adjustments (< 5%) to the uncorrected streamguage data (M. Langland, personal communication, 2004). The Conowingo, Maryland streamguage is ideally situated to capture the influence of freshwater flow on bay salinity, but its record only dates back to 1967. Consequently, a longer (1891–2001), monthly mean discharge record was used from the USGS streamguage at Harrisburg, Pennsylvania, about 100 km upstream. Najjar (1999) found the two streamguage records to be highly correlated ($r^2 = 0.99$), with mean monthly Conowingo flow 14.5% greater than that at Harrisburg. Therefore, we calculated monthly mean discharge at the Susquehanna mouth for the period 1891–2001 by multiplying the Harrisburg values by 1.145. As with salinity data, monthly discharge values were averaged over portions of the year with a focus on spring months. Mean discharge values were calculated over the entire year (annual), MAMJ, MJ, May and June, and again always represent a monthly value.

Monthly precipitation data were obtained from the National Climatic Data Center (NCDC)[1] for the period 1895–2001. Six National Climatic Data Center state divisions in Pennsylvania and New York approximate the Susquehanna watershed (Figure 1). State divisions capture general climate characteristics through a complex combination of representative regional weather stations, and can be used to assess climatic patterns on centennial scales (Karl, 1983; Guttman and Quayle, 1996). Annual monthly MAMJ, MJ, May and June precipitation values were compiled to compare with salinity and discharge records.

Model calibration

The relationship between Susquehanna discharge and CB4.1C salinity during the 17-yr calibration period (1985–2001) was examined using auto and least squares regression (Table 1). The autoregressive model used all temporal (annual, MAMJ, etc.) and spatial (below 20 m and 30 m) divisions of instrumental salinity and discharge data to reconstruct past discharge, with the assumption that present and future values of salinity and discharge statistically represent past discharge. The general equation for the model is:

$$d_t = a_1\, d_{t+1} + a_2\, d_{t+2} + \ldots + a_n\, d_{t+n} + \beta_0 s_t + \beta_1 s_{t+1} + \ldots + \beta_m s_{t+m} + k \quad (1)$$

where d_t is the present annual monthly mean Susquehanna discharge (m^3/s), and s_t is the present annual monthly mean Susquehanna salinity (ppt). Discharge at time t was derived from the preceding n annual monthly mean discharges, the annual monthly mean salinity at t, the preceding m annual monthly mean salinities, and a constant k. Models used an n value of 2, and an m value of 1 to avoid spuriously high correlation coefficients, which varied widely ($r^2 = 0.04$–0.65), but were highest for annual relationships (Table 1a).

Data were also modelled over all temporal and spatial divisions using a least squares curve fit, which assumed discharge was directly influenced by salinity. In order to determine the most appropriate least squares fit, the 17 years of monthly mean salinity, at 20 and 30 m water depths, were plotted against annual, MAMJ, MJ, May and June monthly mean discharge and fit with a variety of trend lines. Power regressions had the highest correlation ($r^2 = 0.17$–0.50), with annual data having the best fit, and the advantage of not computing negative discharge values for anomalously high salinities (Table 1b). The general power regression is:

$$d_t = k s_t^a \quad (2)$$

where d_t is the present monthly mean Susquehanna discharge (m^3/s), s_t is the present annual monthly mean Susquehanna salinity (ppt), and k is a scaling constant.

The relationship between Susquehanna River discharge and watershed precipitation was analysed over a calibration period from 1948 to 2001 using a variety of least squares regressions, assuming discharge was directly related to precipitation. As with salinity–discharge relationships, monthly mean discharge and precipitation were plotted against each other during annual, MAMJ, MJ, May and June periods (Table 1c). Linear regression resulted in the most robust correlations for all spans of time ($r^2 = 0.54$–0.87), with annual relationships again being strongest, and was determined to be the best model of precipitation.

Results

Model verification

Salinity–discharge auto and power regressions were applied to CBI salinity for the verification period of 1950–1979 during corresponding periods of the year at > 20 m and > 30 m water depths. The resulting output was compared with instrumental Susquehanna streamguage data to assess the accuracy of models. Correlation between instrumental records and discharge models varied widely for both autoregression ($r^2 =$ 0.00–0.58) and power regression ($r^2 = 0.10$–0.73), but MJ or June models typically explained the greatest variability (Table 1a, b). With the exception of June autoregression, all 1950–

Table 1 Modelled discharge and precipitation results for all times and depths considered, and their accompanying statistical correlation with instrumental data. Discharge was modelled below both 20 and 30 m water depth (a) autoregressively, and (b) with power regression, while precipitation was modelled with (c) power and linear regression. Boxed discharge models were applied to the RD/2209 palaeosalinity record, and the boxed precipitation model was applied to the resulting modelled discharge

	Calibration period		Verification period			
	1985–2001 salinity–discharge autoregression[a]	1985–2001 salinity–discharge autoregression[b]	r^2 of 1950–1979 instrumental and modelled discharge[a]	r^2 of 1950–1979 instrumental and modelled discharge[b]	RE of 1950–1979 instrumental and modelled discharge[a]	RE of 1950–1979 instrumental and modelled discharge[b]
Salinity–discharge autoregressions						
Annual	$d_t = -0.00934(d_{t+1}) - 153.589(s_t) + 4037.296$ $r^2 = 0.65$	$d_t = -0.00723(d_{t+1}) - 198.518(s_t) + 4935.988$ $r^2 = 0.65$	0.42	0.13	−0.13	−1.72
Mar–Jun	$d_t = -0.00954(d_{t+1}) - 216.148(s_t) + 5802.150$ $r^2 = 0.41$	–	0.00	–	−5.85	–
May–Jun	$d_t = -0.00362(d_{t+1}) - 154.767(s_t) + 3771.411$ $r^2 = 0.24$	$d_t = -0.00348(d_{t+1}) - 168.342(s_t) + 4127.843$ $r^2 = 0.26$	0.45	0.58	−0.24	−0.75
May	$d_t = -0.00142(d_{t+1}) - 156.260(s_t) + 4044.794$ $r^2 = 0.21$	$d_t = -0.00184(d_{t+1}) - 177.211(s_t) + 4554.247$ $r^2 = 0.28$	0.18	0.07	−0.87	−1.63
June	$d_t = -0.00773(d_{t+1}) - 122.211(s_t) + 2975.244$ $r^2 = 0.27$	$d_t = -0.00696(d_{t+1}) - 129.277(s_t) + 3175.303$ $r^2 = 0.25$	0.29	0.51	0.40	0.22
Salinity–discharge power regressions						
Annual	$d_t = 5.40*10^6 s_t^{-2.96}$ $r^2 = 0.56$	$d_t = 1.65*10^7 s_t^{-3.31}$ $r^2 = 0.54$	0.42	0.12	−2.16	−1.34
Mar–Jun	$d_t = 2.71*10^5 s_t^{-1.83}$ $r^2 = 0.32$	$d_t = 1.32*10^6 s_t^{-2.37}$ $r^2 = 0.38$	0.10	0.35	−1.39	1.42
May–Jun	$d_t = 1.25*10^7 s_t^{-3.34}$ $r^2 = 0.37$	$d_t = 1.98*10^6 s_t^{-3.05}$ $r^2 = 0.32$	0.62	0.55	−3.69	−11.19
May	$d_t = 1.83*10^6 s_t^{-2.61}$ $r^2 = 0.33$	$d_t = 2.47*10^6 s_t^{-2.69}$ $r^2 = 0.36$	0.22	0.36	−2.3	−1.84
June	$d_t = 7.85*10^5 s_t^{-2.51}$ $r^2 = 0.19$	$d_t = 6.92*10^5 s_t^{-2.44}$ $r^2 = 0.15$	0.73	0.65	−4.27	−30.34
Discharge–salinity regressions						
Annual	$p_t = 0.0037 d_t + 4.44$ $r^2 = 0.87$	$P_t = 0.31 d_t^{0.4746}$ $r^2 = 0.85$	0.34	0.23		
Mar–Jun	$p_t = 0.003 d_t + 4.07$ $r^2 = 0.59$	$P_t = 0.17 d_t^{0.54}$ $r^2 = 0.56$	0.48	0.29		
Mar–Jun	$p_t = 0.005 d_t + 4.14$ $r^2 = 0.78$	$P_t = 0.16 d_t^{0.59}$ $r^2 = 0.67$	0.84	0.77		
May	$p_t = 0.0046 d_t + 3.204$ $r^2 = 0.54$	$P_t = 0.09 d_t^{0.64}$ $r^2 = 0.46$	0.60	0.34		
June	$p_t = 0.0048 d_t + 5.97$ $r^2 = 0.68$	$P_t = 0.0404 d_t^{0.48}$ $r^2 = 0.46$	0.30	0.06		

[a]Modelled from salinity below 20 m water depth.
[b]Modelled from salinity below 30 m water depth.
–No Mar–June autoregression of salinity below 30 m is included because of a calibration period correlation.

1979 discharge models yielded negative reduction of error statistics (RE) when compared with 1950–1979 instrumental streamguage discharge, suggesting models do not capture verification period variability better than the calibration period mean.

Similarly, instrumental streamguage data was input into discharge–precipitation regressions using a verification period from 1900 to 1948, to produce modelled precipitation. Because they consistently outperformed others in the verification period, linear regressions were the sole equations used to calculate verification period precipitation. Applying linear regressions to instrumental discharge resulted in modelled precipitation records that correlated well with instrumental precipitation ($r^2 = 0.30–0.84$), and were strongest in the MJ period (Table 1c). Positive RE values (0.06–0.77) for all linear regressions indicated they also explained additional variability outside the 1948–2001 calibration period mean.

Recent isotopic palaeosalinity

We applied the best-performing autoregressive and power models to the RD/2209 palaeosalinity record from 1900 to 1996 to assess their potential palaeoclimatic applications. The proximity of core site RD/2209 to monitoring station CB4.1C allowed us to groundtruth the palaeosalinity-based model discharge to a comparable local instrumental record. We analysed three-point running mean values of model-generated and instrumental salinity to minimize the effects of sediment mixing and bioturbation. Statistical tests, including square of the correlation coefficient (r^2), reduction of error statistic (RE) and deviation from instrumental means, must be regarded cautiously as the brief calibration period and small age model errors may impact statistical accuracy. Matching peak discharge events provides a non-statistical means of examining models, and was our primary evaluator.

Two discharge models, D1 and D2, best correlated with instrumental data, and statistical comparisons are summarized in Table 2. Model D1 is an autoregression of annual monthly mean discharge and annual salinity below 20 m water depth (Figure 3a). Inspection of patterns reveals the model captures broad decadal changes in discharge. Ten periods of high discharge, labelled discharge peaks D1P1–10, are identified in both the model and instrumental output. The temporal offset is readily accounted for by smoothing because of sedimentary processes in the core record, and slight errors in radiocarbon dating corrections. Model D1 underestimates some periods of peak discharge by 15% (D1P6) and overestimates others by as much as 46% (D1P3). Model D1 often produces impossible negative discharge values at high salinities, which may be the result of palaeosalinity values outside the range of the 1985–2001calibration period. Statistical analysis of model D1 indicates modelled discharge weakly correlates with 1900–1996 instrumental discharge ($r^2 = 0.21$), though mean values of simulated and instrumental discharge differ by only 10% (Table 2).

Model D2 (Figure 3b) is a power regression of MJ discharge from MJ salinity below 20 m water depth. Sedimentary process smoothing and dating inaccuracies also influence model and instrumental correlation, creating a modest correlation between model D2 and instrumental discharge ($r^2 = 0.37$). D2 deviates from the 1900–1996 instrumental mean by only 19%, and the power regressive form of model D2 places zero limits on both variables to compute a positive discharge for all salinity values. The model captures decadal discharge variations in well-defined peak events D2P1–8, which range from underestimates of 43% (D2P6) to overestimates of 24% (D2P3). Spring Susquehanna discharge is naturally more variable than the annual average (Schubel and Pritchard, 1986), making D2 peaks more extreme and thus easily identified. A spring discharge model may be more appropriate since substituting average May instrumental water temperature into the salinity calculation (Cronin *et al.*, 2000) closely approximates isotopically derived palaeosalinity, supporting data from ecological studies that foraminiferal shell growth is greatest during the spring season. The limited applicability of statistical analyses place greater weight on peak correlation, and easily identified peaks, coupled with a spring signal and inherent positive output, suggest D2 is the better model of Susquehanna discharge.

In order to coordinate with D2, we used the highly correlated linear regression of MJ instrumental discharge and precipitation (calibration $r^2 = 0.78$, verification $r^2 = 0.65$, RE = 0.46) to model precipitation from palaeosalinity (Figure 4). The palaeosalinity-derived D2 discharge record was input into this model, P1, to reconstruct 1900–1996 precipitation and compared with our composite instrumental precipitation record. As with discharge models, sediment processes and age model errors impair statistical correlations, but P1 nevertheless captures a portion of precipitation variability ($r^2 = 0.22$) and deviates from the instrumental mean by a scant 9% (Table 2). More importantly, precipitation peaks derived from D2 discharge, labelled PP1–10, accurately capture the timing of maxima, and range from underestimates of 45% (PP2) to overestimates of 26% (PP9) with an average maxima difference of 20.3%. The statistical correlation with instrumental discharge and well-matched maxima indicate P1 accurately models precipitation, and may be used to reconstruct precipitation from palaeosalinity-derived discharge.

Table 2 Statistical and non-statistical correlation between modelled and instrumental discharge and precipitation. Discharge correlation compares RD/2209 palaeosalinity-derived discharge (D1 and D2) and 1900–1996 USGS instrumental streamguage data. Precipitation correlation compares precipitation modelled from D2 discharge (P1) with our composite instrumental precipitation record.

	Discharge		Precipitation
	Model D1	Model D2	Model P1[a]
Equation	$d_t = -0.00934\ (d_t+1) - 153.589(s_t)+4037.296$	$d_t = 1.25*107s_t^{-3.34}$	$p_t = 0.005\ *d_t+4.14$
r^2 of 1900–1996 instrumental and modelled values	0.21	0.37	0.22
Mean difference[a]	10%	19%	9%
Average maxima difference	24.1%	19.2	20.3%
Range of maxima difference	−15 to 46%	−43 to 24%	−45 to 26%

[a]Uses D2-derived discharge.

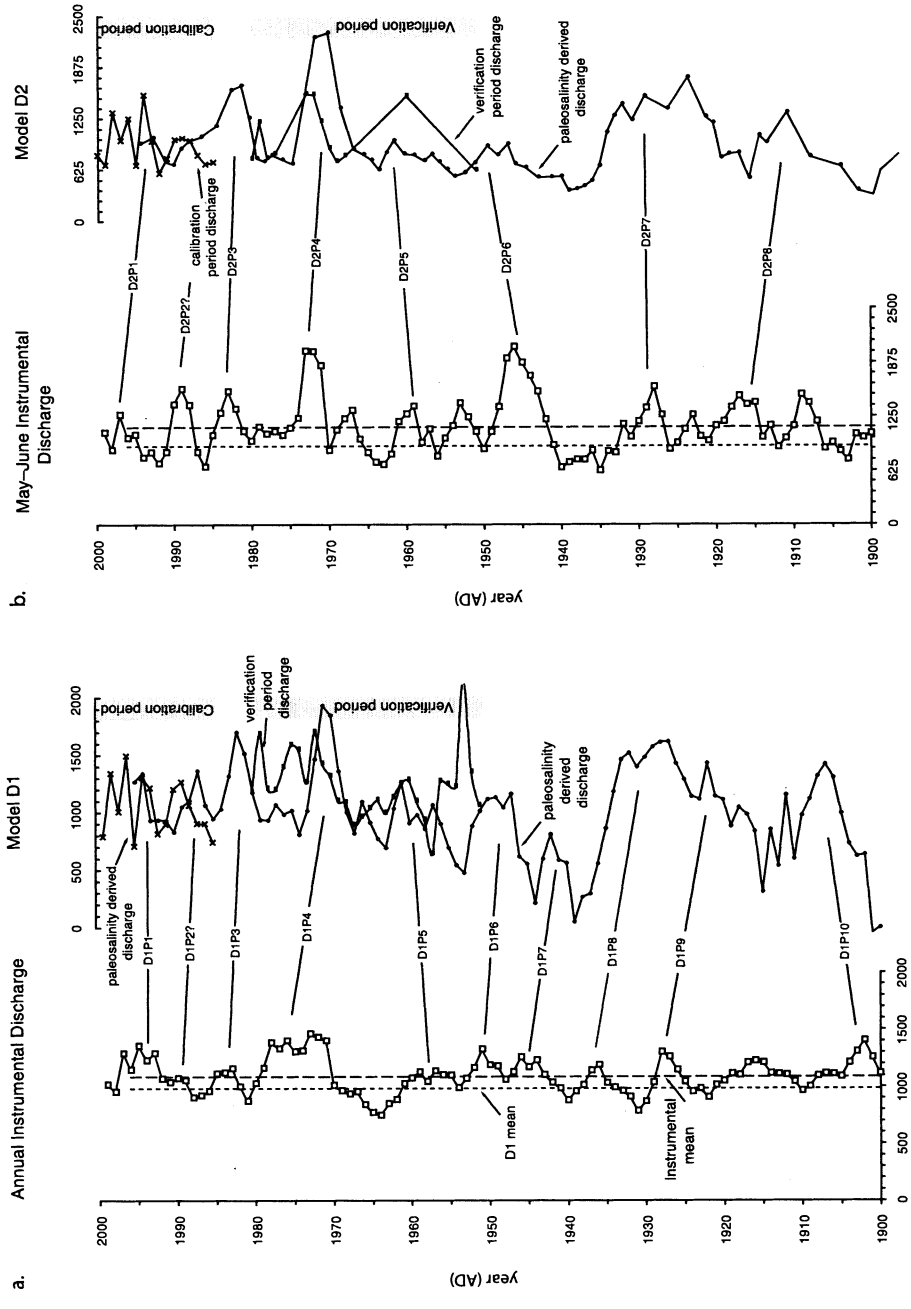

Figure 3 (a) Annual monthly mean Susquehanna discharge (left column, open squares) compared with autoregressive model D1 output (right column, solid circles). D1 was applied to CB4.1C instrumental salinity during the calibration period (1985–2001), verification period (1950–1979) and RD/2209 twentieth-century salinity reconstructions. Peak matching is our primary evaluator, and identifies ten peaks ranging from overestimates of 46% (D1P3) to underestimates of 15% (D1P6). D1 deviation from the instrumental mean is 10%. (b) As for (a) except May–June mean instrumental discharge (left column, open squares) is compared to power regressive model D2 (right column, solid circles). Eight peaks were matched and ranged from overestimates of 24% (D2P3) to underestimates of 43% (D2P6). Peak D2P2, evident in the instrumental record, is not apparent in D2, and D2 deviation from the instrumental mean is 19%

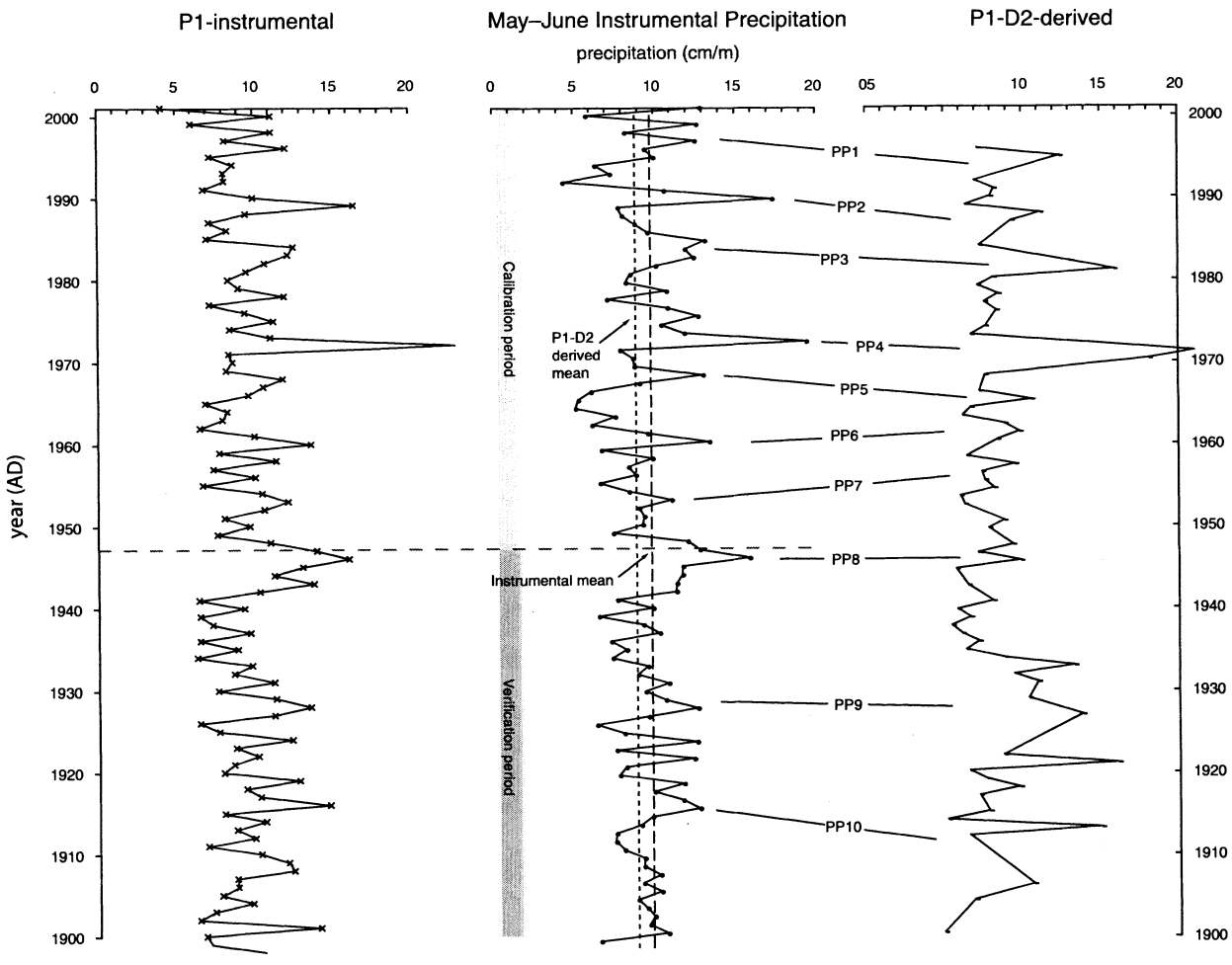

Figure 4 Comparison of modelled (far left and right columns) and instrumental Chesapeake precipitation (centre column). The P1-instrumental model applies linear model P1 to USGS instrumental discharge. P1-D2 derived model applies P1 to D2 discharge output. D2 shows close correlation with instrumental data, and a mean difference of only 9%. Ten peaks were matched ranging from overestimates of 26% (PP9) to underestimates of 45% (PP2)

Holocene isotopic palaeosalinity

We applied models D2 and P1 to the RD/2209 palaeosalinity record to determine if models realistically represent centennial- to millennial-scale patterns of palaeoenvironmental change. RD/2209 palaeosalinity was used for the salinity term in D2, and the resulting D2 output was used as the discharge term in model P1. Smoothed with three-point triangular window, reconstructed discharge and precipitation show identical trends because of the linear nature of P1, but vary realistically from present values.

These model results suggest a drier early–mid Holocene (7055–5900 yr BP) with significantly lower discharge and precipitation (Figure 5), in which reconstructed Susquehanna discharge was ~72% lower (229 m^3/s) than that during the late Holocene (1500 yr BP–present, 820 m^3/s). Precipitation also indicated drier conditions during the early–mid Holocene, and was on average ~36% (5.28 cm/month) lower than during the late Holocene (8.24 cm/month).

The late Holocene palaeoclimate record of models D2 and P1 also seems to capture decadal to centennial variability during the 'Mediaeval Warm Period' (MWP, ~1200–600 yr BP) and the 'Little Ice Age' (LIA, ~600–100 yr BP). Discharge and precipitation during the MWP were lower than twentieth-century means by approximately 11% (810 m^3/s) and 6% (8.19 cm/month), respectively, although abrupt shifts to wetter conditions marked by monthly discharge and precipitation values approaching 1600 m^3/s and 11 cm punctuated the MWP. The LIA was marked by wetter conditions with an estimated 8% greater discharge (979 m^3/s) and 4% greater precipitation (9.03 cm/month).

Discussion

The reconstruction of precipitation based on statistical models and Chesapeake Bay salinity can be evaluated in light of other regional palaeoclimate records and potential forcing of Holocene climate over millennial, centennial and decadal timescales. The first-order trend from drier early Holocene (higher bay salinity) toward wetter (lower salinity) late Holocene conditions is supported by evidence for dry early–mid Holocene conditions in the region, as seen in fossil pollen distributions that indicate drier and warmer conditions around 6000 yr BP (Whitehead, 1971; Watts, 1979; Willard *et al.*, 2005). Our results are also consistent with climate model output showing 20% less precipitation in the Susquehanna basin at 6000 yr BP (Bartlein *et al.*, 1998; Webb *et al.*, 1998) and greater precipitation in the eastern USA since that time (Kutzbach *et al.*, 1998). Within the late Holocene, our record agrees with pollen and dynocyst records from Chesapeake Bay that suggest several centuries of dry conditions during the MWP between ~1200 and 800 yr BP with increasing precipitation after ~500 yr BP (Willard *et al.*, 2003). Increased aridity during the MWP may also be related to multidecadal 'megadroughts' believed to have occurred throughout the central USA prior to 400 yr BP (Woodhouse and Overpeck, 1998). The magnitude of mean

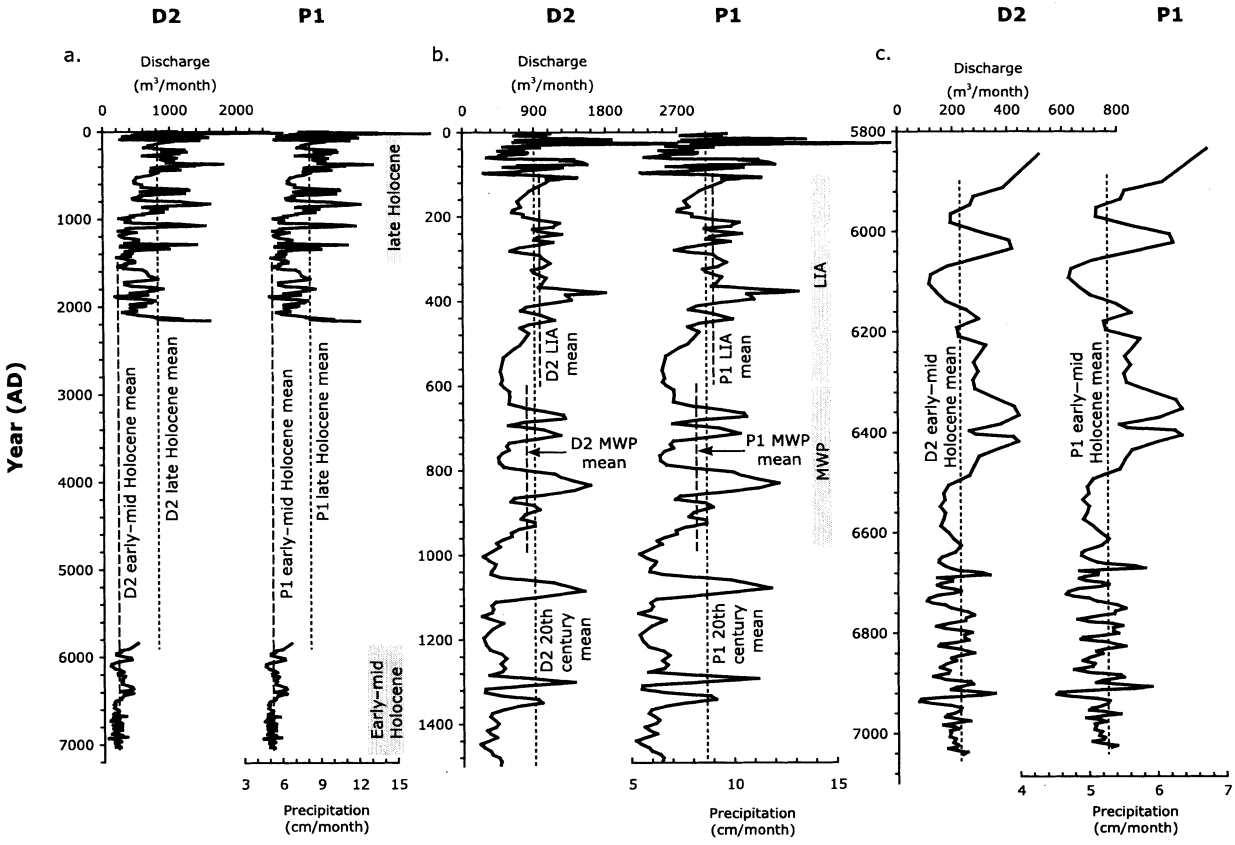

Figure 5 (a) Early–mid and late Holocene three-point smooth of discharge and precipitation as determined by applying D2 and P1 to the 7055 year RD/2209 foraminiferal $\delta^{18}O$-derived palaeosalinity record. The earliest 1200 years of the record (7055–5900 yr BP) show lower mean discharge (229 m^3/s) and precipitation (5.28 cm/month) compared with the late Holocene (1500–0 yr BP) mean discharge (820 m^3/s) and precipitation (8.24 cm/month). Mean values are based on the unsmoothed data. (b) Enlarged view of late-Holocene discharge and precipitation. Comparison with twentieth-century means (907 m^3/s, 8.68 cm/month) indicates a wetter mean LIA (979 m^3/s, 9.03 cm/month), and drier mean MWP (810 m^3/s, 8.19 cm/month). (c) Enlarged view of early–mid Holocene discharge and precipitation. The record shows lower mean values (229 m^3/s, 5.28 cm/month) and lower amplitude variability

changes between the MWP, LIA and present is supported by pollen-based precipitation estimates from the northeastern USA (Gajewski, 1988), and tree ring-derived southeastern US discharge and precipitation reconstructions (Stahle and Cleaveland, 1994; Cleaveland, 2000), which both suggest relatively minor variability ($< \sim 5\%$) in precipitation during the MWP, LIA and the twentieth century.

Rising relative sea level in Chesapeake Bay is one hypothesis to account for long-term Holocene salinity changes. Although this factor cannot be completely ruled out, relative sea level reached within ~ 5 m of its modern position quite abruptly by ~ 7.5 ka, mainly as a result of glacio-eustatic sea level rise of 15–20 m during the final major phase of global deglaciation (Vogt *et al.*, 2000; Bratton *et al.*, 2003). Conversely, since 7.5 ka, the gradual rise in relative sea level in the bay was the result of postglacial isostatic subsidence in the middle-Atlantic USA, which is located in the peripheral bulge outside regions glaciated by the Laurentide Ice Sheet (Peltier, 1996). Only minimal glacio-eustatic sea-level rise occurred since ~ 7.5 ka. Thus the bay had reached its present approximate modern bathymetric configuration by ~ 7.5 ka when freshwater inflow from the Susquehanna River and other bay tributaries began to drive density-driven circulation.

Changes in coupled ocean–atmosphere dynamics present a second possible mechanism to account for observed precipitation variability in the Susquehanna watershed. Previous studies of eastern US precipitation have called on the interconnection between the North Atlantic Ocean and atmosphere embodied in the positive and negative phases of the NAO (eg, Vega *et al.*, 1999), which strongly influence the convergence of atmospheric moisture and, subsequently, regional precipitation (Hurrell, 1995; Visbeck *et al.*, 2001). While most evident during winter months, the NAO is the dominant climate mode throughout the year, except early autumn, and may heavily influence spring precipitation in the Susquehanna watershed (Rogers, 1990; Portis *et al.*, 2001). High NAO indexes, marked by sharp SLP gradients, encourage zonal circulation, strengthened westerlies and more frequent storms across the middle-Atlantic USA (Hurrell, 1995; Visbeck *et al.*, 2001) Conversely, low NAO indexes are marked by decreased westerlies and meridional circulation (Hurrell, 1995), which cause increased blocking and a southward shift of the mean stormtrack in association with a southerly shifted Gulf Stream (Colucci, 1976; Rogers, 1990). The negative phase of the NAO has been correlated with this nearly due east Gulf Stream orientation, and may result from a strengthening of the cold Labrador current flowing south along the western Atlantic boundary (Rossby and Benway, 2000). While not statistically evident over annual periods, this climatic pattern has been correlated to regional climate on decadal timescales (Hartley and Keables, 1998) and suggests the NAO may be positively correlated with middle-Atlantic US precipitation.

Pacific Ocean–atmosphere interactions have also been considered as a possible source for eastern USA precipitation variability (eg, Leathers *et al.*, 1991; Montroy, 1997), and may further explain changes in precipitation within the Susquehanna watershed. The positive phase of the PNA amplifies trough development over the eastern USA, and causes drier

conditions (Sheridan, 2003). Similarly, increased NPM activity causes stationary wave flux across North America, which results in equivalent-barotropic cyclonic circulation over the northeastern USA and the blocking of normal moisture influx (Barlow *et al.*, 2001). The extent of stationary wave penetration is amplified during negative NAO periods (Barlow *et al.*, 2001), suggesting coupled Atlantic and Pacific Ocean influence on middle-Atlantic precipitation.

The ultimate forcing of NAO and Pacific teleconnection variability through the Holocene is unclear and model results suggest atmospheric, oceanic or coupled systems all have the potential to cause decadal to multicentennial variability (Latif and Barnett, 1994; Goodman and Marshall, 1999; Delworth and Mann, 2000; Garric and Huber, 2003). Further potential sources of variability come from volcanic activity, sea-ice dynamics or changes in solar irradiance (Hakkinen and Geiger, 2000; Shindell *et al.*, 2001). Applying the techniques outlined here to estimate meteorological conditions from sedimentary palaeoclimate archives in other coastal regions should result in a much-improved understanding of the long-term relationship between the ocean–atmosphere teleconnections and regional precipitation patterns.

Conclusion

Quantitative modelling of Chesapeake Bay salinity, Susquehanna River discharge and regional precipitation suggests that simple power and linear regressions adequately reconstruct discharge and precipitation from instrumental and palaeosalinity records, but that autoregression, while useful for projections, may not be as well suited for palaeoclimate reconstruction. Our results suggest that linear and power models successfully capture a first order approximation of regional precipitation variability over centennial to millennial timescales. Model output shows that in the eastern USA, the early–mid Holocene was significantly drier than the late Holocene, and that higher frequency rainfall variability characterized the 'Mediaeval Warm Period' and the 'Little Ice Age'. Shifts in precipitation may be related to Atlantic and Pacific ocean–atmosphere interactions, and the NAO, PNA or NPM. Application of these modelling techniques to millennial-scale climate variability in other regions, where precipitation and salinity are closely related, may allow a more complete evaluation of the interrelation between large-scale atmospheric circulation patterns and regional precipitation, as well as twentieth-century climate patterns in light of anthropogenic and natural forcings.

Acknowledgements

Our thanks to Ray Najjar and Mike Langland for their advice and input, and to Eric Tappa and Gary Dwyer for assistance with isotopic analysis. We greatly appreciate the assistance of the crew and staff of the R/V Marion Dufresne and IMAGES V program. Further appreciation to Ricky Bahner for Chesapeake Bay data management. Additional thanks to two anonymous reviewers and to Chris Bernhardt and Harry Jenter for presubmission revision.

Note

1. Please refer to http://geology.er.usgs.gov/eespteam/Atlantic/climvari.htm for online instrumental data sources, data evaluations and previous precipitation models within the Susquehanna River watershed.

References

Barlow, M., Nigam, S. and **Berbery, E.H.** 2001: ENSO, Pacific decadal variability, and U.S. summertime precipitation, drought, and stream flow. *Journal of Climate* 14, 2105–28.

Bartlein, P.J., Anderson, K.H., Anderson, P.M., Edwards, M.E., Mock, C.J., Thompson, R.S., Webb, R.S. and **Whitlock, C.** 1998: Paleoclimate simulations for North America over the past 21,000 years: features of the simulated climate and comparisons with paleoenvironmental data. *Quaternary Science Reviews* 17, 549–85.

Bradbury, J.A., Keim, B.D. and **Wake, C.P.** 2002: U.S. East Coast trough indices at 500 hPa and New England winter climate variability. *Journal of Climate* 15, 3509–17.

Bratton, J.F., Colman, S.M.E., Thieler, R. and **Seal, R.R., II** 2003: Birth of the modern Chesapeake Bay estuary 7,400 to 8,200 years ago and implications for global sea-level rise. *Geo-Marine Letters*, 22, 188–97.

Broecker, W.S. 1989: The salinity contrast between the Atlantic and Pacific Oceans during glacial time. *Paleoceanography* 4, 207–12.

Cayan, D.R. and **Peterson, D.H.** 1993: Spring climate and salinity in the San-Francisco Bay estuary. *Water Resources Research* 29, 293–303.

Cleaveland, M.K. 2000: A 963-year reconstruction of summer (JJA) streamflow in the White River, Arkansas, USA, from tree-rings. *The Holocene* 10, 33–41.

Cohen, S. and **Miller, K.** 2001: North America. In Waston, R.T., editor, *Climate change 2001: impacts, adaptation and vulnerability.* Intergovernmental Panel on Climate Change Working Group II. Third Assessment Report. Cambridge University Press, 733–800.

Colucci, S.J. 1976: Winter cyclone frequencies over the eastern United States and adjacent western Atlantic 1964–1973. *Bulletin of the American Meteorological Society* 57, 548–53.

Cook, E.R. and **Jacoby, G.C.** 1983: Potomac River streamflow since 1730 as reconstructed by tree rings. *Journal of Applied Meteorology* 22, 1659–72.

Cronin, T., Willard, D., Karlsen, A., Ishman, S., Verardo, S., McGeehin, J., Kerhin, R., Holmes, C., Colman, S. and **Zimmerman, A.** 2000: Climatic variability in the eastern United States over the past millennium from Chesapeake Bay sediments. *Geology* 28, 3–6.

Cronin, T.M., Dwyer, G.S., Kamiya, T., Schwede, S. and **Willard, D.A.** 2003: Medieval Warm Period, Little Ice Age and 20th century temperature variability from Chesapeake Bay. *Global and Planetary Change* 36, 17–29.

Cronin, T.M., Thunnell, R., Dwyer, G.S., Saenger, C., Mann, M.E., Vann, C. and **Seal, R.** 2005: Multiproxy evidence of Holocene climate variability from estuarine sediments, eastern North America. *Paleoceanography* 20, PA4006, doi:10.1029/2005PA001145.

Delworth, T.L. and **Mann, M.E.** 2000: Observed and simulated multidecadal variability in the Northern Hemisphere. *Climate Dynamics* 16, 661–76.

Druckenbrod, D.L., Mann, M.E., Stahle, D.W., Cleaveland, M.K., Therrell, M.D. and **Shugart, H.H.** 2003: Late-eighteenth-century precipitation reconstructions from James Madison's Montpelier plantation. *Bulletin of the American Meteorological Society* 84, 57–71.

Dwyer, G.S. and **Cronin, T.** 2001: Ostracode shell chemistry as a paleosalinity proxy in Florida Bay. In Wardlaw, B., editor, Paleoecological studies of South Florida. *Bulletins of American Paleontology* 361, 249–76.

Epstein, S., Buchsbaum, R., Lowenstam, H.A. and **Urey, H.C.** 1953: Revised carbonate-water isotopic temperature scale. *Geological Society of America Bulletin* 64, 1315–26.

Gajewski, K. 1988: Late Holocene climate changes in eastern North-America estimated from pollen data. *Quaternary Research* 29, 255–62.

Garric, G. and **Huber, M.** 2003: Quasi-decadal variability in paleoclimate records: sunspot cycles or intrinsic oscillations? *Paleoceanography* 18, 1068–76.

Goodman, J. and **Marshall, J.** 1999: A model of decadal middle-latitude atmosphere–ocean coupled modes. *Journal of Climate* 12, 621–41.

Guttman, N.B. and **Quayle, R.G.** 1996: A historical perspective of US climate divisions. *Bulletin of the American Meteorological Society* 77, 293–303.

Hakkinen, S. and **Geiger, C.A.** 2000: Simulated low-frequency modes of circulation in the Arctic Ocean. *Journal of Geophysical Research-Oceans* 105, 6549–64.

Hartley, S. and **Keables, M.J.** 1998: Synoptic associations of winter climate and snowfall variability in New England, USA, 1950–1992. *International Journal of Climatology* 18, 281–98.

Hurrell, J.W. 1995: Decadal trends in the North-Atlantic Oscillation – regional temperatures and precipitation. *Science* 269, 676–79.

Ingram, B.L., Ingle, J.C. and **Conrad, M.E.** 1996: Stable isotope record of late Holocene salinity and river discharge in San Francisco Bay, California. *Earth and Planetary Science Letters* 141, 237–47.

Karl, T.R. 1983: Some spatial characteristics of drought duration in the United States. *Journal of Climate Applications and Meteorology* 22, 1356–66.

Karl, T.R. and **Riebsame, W.E.** 1989: The impact of decadal fluctuations in mean precipitation and temperature on runoff: a sensitivity study over the United States. *Climatic Change* 15, 423–47.

Karl, T.R., Knight, R.W. and **Plummer, N.** 1995: Trends in high-frequency climate variability in the 20th-century. *Nature* 377, 217–20.

Kutzbach, J., Gallimore, R., Harrison, S., Behling, P., Selin, R. and **Laarif, F.** 1998: Climate and biome simulations for the past 21,000 years. *Quaternary Science Reviews* 17, 473–506.

Laird, K.R., Fritz, S.C., Maasch, K.A. and **Cumming, B.F.** 1996: Greater drought intensity and frequency before AD 1200 in the Northern Great Plains, USA. *Nature* 384, 552–54.

Latif, M. and **Barnett, T.P.** 1994: Causes of decadal climate variability over the North Pacific and North America. *Science* 266, 634–37.

Leathers, D.J., Yarnal, B. and **Palecki, M.A.** 1991: The Pacific/North American teleconnection pattern and United States climate. Part I: regional temperature and precipitation associations. *Journal of Climate* 4, 517–28.

Montroy, D.L. 1997: Linear relation of central and eastern North American precipitation to tropical Pacific sea surface temperature anomalies. *Journal of Climate* 10, 541–58.

Najjar, R.G. 1999: The water balance of the Susquehanna River Basin and its response to climate change. *Journal of Hydrology* 219, 7–19.

Peltier, W.R. 1996: Global sea level rise and glacial isostatic adjustment: an analysis of data from the east coast of North America. *Geophysical Research Letters* 23, 717–20.

Peterson, D., Cayan, D., Dileo, J., Noble, M. and **Dettinger, M.** 1995: The role of climate in estuarine variability. *American Scientist* 83, 58–67.

Portis, D.H., Walsh, J.E., Hamly, M.E. and **Lamb, P.** 2001: Seasonality of the North Atlantic Oscillation. *Journal of Climate* 14, 2069–78.

Resio, D.T. and **Hayden, B.P.** 1975: Recent secular variations in mid-Atlantic winter extratropical storm climate. *Journal of Applied Meteorology* 14, 1223–34.

Rogers, J.C. 1990: Patterns of low-frequency monthly sea level pressure variability (1899–1986) and associated wave cyclone frequencies. *Journal of Climate* 3, 1364–79.

Rossby, T. and **Benway, R.L.** 2000: Slow variations in mean path of the Gulf Stream east of Cape Hatteras. *Geophysical Research Letters* 27, 117–20.

Schubel, J.R. and **Pritchard, D.W.** 1986: Responses of upper Chesapeake Bay to variations in discharge of the Susquehanna River. *Estuaries* 9, 236–49.

Sheridan, S.C. 2003: North American weather-type frequency and teleconnections indices. *International Journal of Climatology* 23, 27–45.

Shindell, D.T., Schmidt, G.A., Mann, M.E., Rind, D. and **Waple, A.** 2001: Solar forcing of regional climate change during the maunder minimum. *Science* 294, 2149–52.

Stahle, D.W. and **Cleaveland, M.K.** 1994: Tree-ring reconstructed rainfall over the Southeastern USA during the Medieval Warm Period and Little Ice-Age. *Climatic Change* 26, 199–212.

Stahle, D.W., Cleaveland, M.K., Blanton, D.B., Therrell, M.D. and **Gay, D.A.** 1998: The Lost Colony and Jamestown droughts. *Science* 280, 564–67.

Swart, P.K., Healy, G.F., Dodge, R.E., Kramer, P., Hudson, J.H., Halley, R.B. and **Robblee, M.B.** 1996: The stable oxygen and carbon isotopic record from a coral growing in Florida Bay: a 160 year record of climatic and anthropogenic influence. *Palaeogeography Palaeoclimatology Palaeoecology* 123, 219–37.

Vega, A.J., Sui, C.H. and **Lau, K.M.** 1998: Interannual to interdecadal variations of the regionalized surface climate of the United States and relationships to generalized flow parameters. *Physical Geography* 19, 271–91.

Vega, A.J., Rohli, R.V. and **Sui, C.H.** 1999: Climatic relationships to Chesapeake Bay salinity during Southern Oscillation extremes. *Physical Geography* 20, 468–90.

Visbeck, M.H., Hurrell, J.W., Polvani, L. and **Cullen, H.M.** 2001: The North Atlantic Oscillation: past, present, and future. *Proceedings of the National Academy of Sciences of the United States of America* 98, 12876–77.

Vogt, P.R., Halka, J.P., Hagen, R. and **Cronin, T.** 2000: Geophysical environments in Chesapeake Bay: *Marion-Dufresne* sites MD-2205, 2206, and 2208. In Cronin, T.M., editor, *Initial report on IMAGES V cruise of* Marion-Dufresne *to the Chesapeake Bay, June 20–22, 1999*. U.S. Geological Survey Open File Report 00–306, 18–31.

Wallace, J.M. and **Gutzler, D.S.** 1981: Teleconnections in the geopotential height field during the northern hemisphere winter. *Monthly Weather Review* 109, 784–812.

Watts, W.A. 1979: Late Quaternary vegetation of central Appalachia and New Jersey coastal plain. *Ecological Monographs* 49, 427–69.

Webb, T., Anderson, K.H., Bartlein, P.J. and **Webb, R.S.** 1998: Late quaternary climate change in eastern North America: a comparison of pollen-derived estimates with climate model results. *Quaternary Science Reviews* 17, 587–606.

Whitehead, D.R. 1971: Developmental and environmental history of the dismal swamp. *Ecological Monographs* 42, 301–14.

Willard, D.A., Cronin, T.M. and **Verardo, S.** 2003: Late-Holocene climate and ecosystem history from Chesapeake Bay sediment cores, USA. *The Holocene* 13, 201–14.

Willard, D.A., Bernhardt, C.E., Korejwo, D.A. and **Meyers, S.R.** 2005: Impact of millennial-scale Holocene climate variability on eastern North American terrestrial ecosystems: pollen-based climatic reconstruction. *Global and Planetary Change* 47, 17–35.

Woodhouse, C.A. and **Overpeck, J.T.** 1998: 2000 years of drought variability in the central United States. *Bulletin of the American Meteorological Society* 79, 2693–714.

Yarnal, B. and **Leathers, D.J.** 1988: Relationships between inter-decadal and interannual climatic variations and their effect on Pennsylvania climate. *Annual Association of American Geography* 78, 624–41.